



MATHEMATICAL MODEL FOR MEASURING THE CONCENTRATION OF NANOPARTICLES IN A LIQUID DURING SEDIMENTATION

Safaa Mohammed Ridha Hussien Hussien
University of Karbala, Karbala, Iraq, safaa_m333@yahoo.com

Airat Sakhabutdinov
Kazan National Research Technical University n.a. A.N. Tupolev-KAI, Kazan, Russian Federation, kazanboy@yandex.ru

Vladimir Anfinogentov
Kazan National Research Technical University n.a. A.N. Tupolev-KAI, Kazan, Russian Federation, v.anfinogentov@yandex.ru

Maxim Danilaev
Kazan National Research Technical University n.a. A.N. Tupolev-KAI, Kazan, Russian Federation, danilaev@mail.ru

Vladimir Kuklin
Kazan (Volga) Federal University, Kazan, Russian Federation, iamkvova@gmail.com

See next page for additional authors

Follow this and additional works at: <https://kijoms.uokerbala.edu.iq/home>

 Part of the [Chemistry Commons](#), [Nanoscience and Nanotechnology Commons](#), and the [Physics Commons](#)

Recommended Citation

Hussien, Safaa Mohammed Ridha Hussien; Sakhabutdinov, Airat; Anfinogentov, Vladimir; Danilaev, Maxim; Kuklin, Vladimir; and Morozov, Oleg (2021) "MATHEMATICAL MODEL FOR MEASURING THE CONCENTRATION OF NANOPARTICLES IN A LIQUID DURING SEDIMENTATION," *Karbala International Journal of Modern Science*: Vol. 7 : Iss. 2 , Article 7.

Available at: <https://doi.org/10.33640/2405-609X.2973>

This Research Paper is brought to you for free and open access by Karbala International Journal of Modern Science. It has been accepted for inclusion in Karbala International Journal of Modern Science by an authorized editor of Karbala International Journal of Modern Science. For more information, please contact abdulateef1962@gmail.com.

MATHEMATICAL MODEL FOR MEASURING THE CONCENTRATION OF NANOPARTICLES IN A LIQUID DURING SEDIMENTATION

Abstract

Expanding the application areas of polymer composite materials with dispersed filler requires the development of technologies providing the required mechanical characteristics. One of these methods is based on forming a thin polymer shell on the surfaces of particles. At the same time, it is impossible to take into account the mechanical characteristics of a thin polymer shell due to its ultra-small thickness. The mechanical properties of the polymer shell can be determined only by indirect methods, and prior information can improve the adequacy of the properties determination. The method, which allows reducing the requirements for composite sample preparation, is proposed. This method is based on the sedimentation approach. It is suggested to evaluate the sedimentation time (or velocity) by measuring the optical density of the solution, consisting of nanoparticles and polymer macromolecules. The nanoparticle and polymer macromolecules parameters are defined using sedimentation time. The mathematical model for simulation of the photo sedimentation velocity of particles in a solvent is developed. The model considers the sedimentation process under the influence of gravity, hydrostatic lift, and drag forces. The model takes into account also the influence of the Brownian motion of the solvent on the particle movements based on elastic collision as well as the effect of the inelastic collision of particles with each other. The particle concentration is estimated based on beam light scattering modeling. The results of the mathematical model investigation and the experimental results confirm the feasibility of the proposed method. The results and estimations allow both to determine the sedimentation time and to formulate the method requirements for measuring particles of various sizes and densities. The proposed approach can be used to create equipment for nanoparticle parameters (mass, density) measuring.

Keywords

sedimentation, particle sedimentation in liquid, molecular mass measurement, nanoparticle measurement, concentration measurement, Rayleigh scattering

Creative Commons License



This work is licensed under a [Creative Commons Attribution-Noncommercial-No Derivative Works 4.0 License](https://creativecommons.org/licenses/by-nc-nd/4.0/).

Cover Page Footnote

A.Zh. Sakhabutdinov and O.G. Morozov were funded by the Ministry of Science and Higher Education of the Russian Federation Agreement № 075-03-2020-051 (fzsu-2020-0020, FOKRAT) in part of physical task formulation, data, and verification of results. M.P. Danilaev and V.A.Kuklin were funded by the Ministry of Science and Higher Education of the Russian Federation Agreement No. 075-03-2020-051/3 from 09.06.2020 (fzsu-2020-0021) in part of the mathematical model construction, training and tuning, and realization.

Authors

Safaa Mohammed Ridha Hussien Hussien, Airat Sakhabutdinov, Vladimir Anfinogentov, Maxim Danilaev, Vladimir Kuklin, and Oleg Morozov

1. Introduction

Expanding the application areas of polymer composite materials with dispersed filler requires the development of technologies providing the required mechanical characteristics. The various kinds of fibers as a filler, such as nanofibers [1] and microfibers, single-wall carbon nanotubes [2], multi-wall carbon fiber [3], single carbon black [4], carbon nanotubes [5,6] are being studied. The research of mathematical models of such materials makes it possible to formulate requirements for the particles of polymer and filler [7,8]. However, investigating the mathematical models using numerical methods, requires information about the mechanical properties of each of the composition components [9,10]. It should be noted that the mechanical properties of the entire polymer composition are determined not only by the mechanical properties of each component but also by the degree of interaction of the nanoparticles with the polymer matrix [11]. To improve this interaction, the surface of the particles is modified by various methods [12,13]. One of these methods is based on forming a thin polymer shell on the surfaces of particles [12]. At the same time, it is impossible to take into account the mechanical characteristics of a thin polymer shell when a mathematical model of composite is studied. This is due to the fact that a typical thickness of the polymer shell is about 10–100 nm, so it is impossible to measure its mechanical properties directly. The mechanical properties of the polymer shell can be determined only by indirect methods, the main of which is the solution of the inverse task of mechanics of polymer. A wide range of properties of polymer composite materials, measurement errors, limitations, and assumptions of mathematical models do not allow ensuring the adequacy and uniqueness of the solution of inverse tasks in this case [14]. Even any a priori information can improve the adequacy of the solution and reduce the range of the solutions of the inverse tasks. For example, it is possible to estimate the mechanical properties of a polymer shell on the surfaces of particles knowing the molecular weight of the polymer and its density.

Currently, there are many proven methods for measuring the molecular weight of a polymer. So, in the works [15–17] the main methods for measuring the molecular weight of a polymer in a wide dynamic range are discussed in detail. However, the use of these

methods requires the separation of nanoparticles and polymer molecules. This separation can be realized in solutions using polymer shell solvent. Moreover, it can be done either before the experiment, for example, in centrifuges [18,19], or during the experiment, for example, using the sedimentation methods [20,21].

The method, which allows reducing the requirements for composite sample preparation, is proposed in this work. It is suggested to control the sedimentation velocity by measuring the change in the optical density of the solution, consisting of two types of particles (nanoparticles and polymer macromolecules). It is possible to estimate some mechanical characteristics of the polymer, for example, the modulus of elasticity, Poisson's ratio from the known values of the molecular weight and packing density of polymer molecules [22,23]. The mathematical model for approximation of the photo sedimentation velocity of two types of particles is proposed. The assessment of the adequacy of the model is evaluated by comparing the simulation results with the experimental data.

2. Task formulation

The measurement system consists of a quartz container with a solvent, Fig. 1, *a*. The filler particles (aluminum oxide) coated with polymer fibers are placed in the solvent (ethyl acetate) and shaken. The particles of filler and polymer macromolecules are separated in a solvent. The particles begin to sediment only under the influence of gravity. It is assumed that the depositing nanoparticles of both the filler and the shell are electrically neutral. Therefore, the forces of electrostatic interaction can be neglected. The measurement of a particle's concentration is based on the analysis of Rayleigh scattering.

The laser ray is beamed at the face of the quartz container, and a photodetector is installed at the other end. The output current of the photodetector is inversely proportional to the concentration of the particles. Over time, the particles are sedimented, and the total light transmitted through the container is changed. Basing on the light beam intensity change, it is possible to make a conclusion about the current concentration of the particles in the liquid [12,24]. The task is to simulate the change of the optical power of the light beam passing through the quartz container during the sedimentation of the particles.

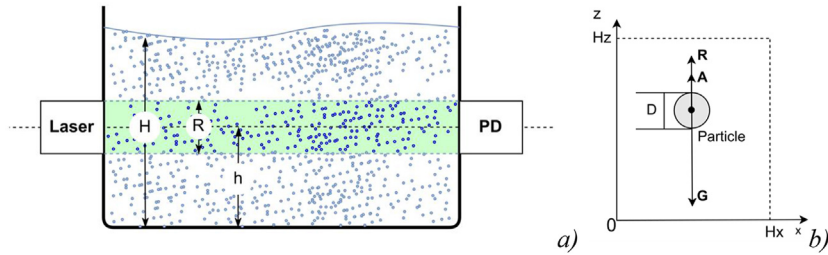


Fig. 1. The measurement system scheme (a); the forces acting on the particle in a liquid (b); \mathbf{G} is the gravity force, \mathbf{A} is the Archimedes force, \mathbf{R} is liquid resistance force, D is the diameter of the particle.

3. Mathematical model

3.1. The equation of motion of a particle

The motion of a particle in a liquid under the gravity, hydrostatic lift, and liquid resistance forces is described by the equation:

$$M_i \frac{d\mathbf{W}_i}{dT} = \mathbf{G}_i - \mathbf{A}_i - \mathbf{R}_i, \quad (1)$$

where \mathbf{A}_i – Archimedes, \mathbf{G}_i – gravity, \mathbf{R}_i – liquid resistance are forces vectors, \mathbf{W}_i is velocity vector, M_i is a mass of a particle, and T is time; the subscript index “ i ” indicates an individual particle.

The gravity force is:

$$\mathbf{G}_i = M_i \mathbf{g}, \quad (2)$$

where \mathbf{g} is the vector of gravitational constant.

The force of Archimedes is directed in the opposite direction to the gravity vector and is equal to the weight of a liquid displaced by a particle:

$$\mathbf{A}_i = -V_i \rho \mathbf{g} = -\frac{\pi}{6} D_i^3 \rho \mathbf{g}, \quad (3)$$

where V_i is volume, D_i is diameter of a particle, and ρ is density of liquid.

The liquid resistance force is directed against the particle velocity. It depends on the square of the particle velocity, the liquid density, the particle cross-sectional area, and the Reynolds number (Re). The latter is determined by the particle velocity and the viscosity of the liquid:

$$R_i = -\xi(\text{Re}) \frac{\rho W_i^2}{2} S_i, \text{ where } \xi(\text{Re}) = \frac{24}{\text{Re}} \text{ and} \quad (4)$$

$$\text{Re} = \frac{W_i D_i \rho}{\mu}$$

where $\xi(\text{Re})$ is dimensionless coefficient depending on Re for low-speed motions, S_i is particle cross-sectional

area, μ is dynamic viscosity coefficient of a liquid. The cross-sectional area for a spherical particle with diameter D_i is:

$$S_i = \pi \frac{D_i^2}{4}. \quad (5)$$

Therefore, the liquid resistance force can be written as:

$$R_i = -\frac{24}{\text{Re}} \frac{\rho W_i^2}{2} S_i = -\frac{24\mu}{W_i D_i \rho} \frac{\rho W_i^2}{2} \pi \frac{D_i^2}{4} = -3\mu\pi D_i W_i. \quad (6)$$

It should be noted, that the hydrodynamic radius of the particle is used in Equations (1)–(6) to take into account interfacial tension indirectly.

Particles can be acted upon not only by gravity, but also by Brownian (thermal) motion of liquid molecules [25,26]. The velocity of Brownian motion depends only on the ambient temperature. Let us define the temperature near the particle as the linearly varying temperature between the upper and lower boundaries of the container:

$$K_i = K_T + \frac{(K_B - K_T)}{H} z_i, \quad (7)$$

where K_T is a top and K_B is a bottom surface temperature.

3.2. The model of Brownian influence

The model of elastic collision of a particle with mass m_i and velocity w_i with a molecule of a liquid with the average mass m and the average velocity w can be described as:

$$w_i^B = \frac{w_i(m_i - m) + 2mw}{m_i + m}. \quad (8)$$

The average kinetic energy of a molecule of a liquid is related to the Avogadro number N_A by the relations [27]:

$$E = \frac{mw^2}{2}, N_A = \frac{3RK}{2E} \text{ and } m = \frac{M_O}{N_A} \tag{9}$$

where K is a temperature and E is an average kinetic energy of molecules of a liquid, M_O is a molar mass of a liquid. The velocity taken by a particle under the Brownian motion of a liquid is:

$$w_i^B = \frac{(N_A m_i - M_O)w_i + 2\sqrt{3}\Re M_O \cdot \left(\text{rnd}(1) - \frac{1}{2}\right)}{N_A m_i + M_O}, \tag{10}$$

where \Re is universal gas constant. The factor $(\text{rnd}(1) - 1/2)$ was added in (10) to introduce a random character of Brownian collisions. The whole Brownian velocity is:

$$w_i^{BW} = \frac{(N_A m_i - M_O)w_i + 2\sqrt{3}\Re M_O}{N_A m_i + M_O}, \tag{11}$$

3.3. The model of light obscured by particles

Denoting the height of the quartz container as H , we describe the laser beam passing through the container as a round cylinder of radius R located at a height of h . Then the total light flux obscured by the particles can be described as:

$$S(t) = \chi \sum_{i=1}^{N_1+N_2} \frac{\pi d_i^2}{4} \sqrt{1 - \left(\frac{z_i - h}{R}\right)^2}, \tag{12}$$

where $h - R < z_i < h + R$

where d_i is a diameter, z_i is coordinate of a particle, χ is aspect ratio.

3.4. The model of particle collisions

When two particles with coordinates z_i and z_j and velocities w_i and w_j are close to each other, there is a nonzero chance to their inelastic collision. The condition of collision can be written as:

$$(w_i + w_j) \cdot \Delta t \leq d_i + d_j. \tag{13}$$

The probability of collision can be calculated as the relation of areas:

$$p_{ij} = \frac{\pi \left(w_i^{BH}\right)^2 + \left(w_j^{BH}\right)^2}{S_H}, \tag{14}$$

where S_H is an area of horizontal surface of the container, and w_i^{BH} is the velocity of a particle in horizontal plane, which can be calculated as:

$$w_i^{BH} = \sqrt{\left(w_i^{BW}\right)^2 - \left(w_i^B\right)^2}. \tag{15}$$

If the probability of collision p_{ij} is greater than arbitrary random value, we assume that collision takes place.

The inelastic collision assumes that particles stick together. Let us assume that after collision the i -th particle obtains a new mass, velocity, and diameter, and j -th particle disappears. Thus, the i -th particle with a new mass appears:

$$\hat{m}_i = m_i + m_j. \tag{16}$$

New velocity, diameter, and coordinate can be calculated by:

$$\hat{w}_i = \frac{m_i w_i + m_j w_j}{m_i + m_j}, \hat{d}_i = \sqrt[3]{d_i^3 + d_j^3}, \text{ and } \hat{z}_i = \frac{z_i + z_j}{2}. \tag{17}$$

New mass, velocity, diameter and coordinate for j -th particle are equal to zero.

4. Equations of particles motion in dimensionless form

The equation of motion of the particle (1), after substituting (2), (3) and (6) into it, takes the form:

$$M_i \frac{dW_i}{dT} = M_i g - \frac{\pi}{6} D_i^3 \rho g - 3\mu\pi D_i W_i \tag{18}$$

Let us transform equation (18) into dimensionless form using characteristic parameters of the task, namely: characteristic size (L_0), mass (M_0), time (T_0), and temperature (K_0). The absolute values of characteristic parameters of the task can be selected from the values of the physical quantities of the task. Let us introduce the dimensionless variables: w – velocity, m – mass, d – diameter and τ – time. The dependencies between dimensional and dimensionless variables will be written as:

$$\begin{aligned} W_i &= \frac{dZ_i}{dT} = \frac{d(L_0 \times z_i)}{d(T_0 \times \tau)} = \frac{L_0}{T_0} \times w_i \\ D_i &= L_0 \times d_i \\ M_i &= M_0 \times m_i \\ T &= T_0 \times \tau \end{aligned} \tag{19}$$

The final dimensionless equation takes the form:

$$\frac{M_0 L_0}{T_0^2} m_i \frac{d}{d\tau} w_i = M_0 m_i g - \frac{\pi}{6} L_0^3 d_i^3 \rho g - 3\pi\mu \frac{L_0^2}{T_0} d_i w_i, \tag{20}$$

or, introducing the notation for dimensionless complexes:

$$\mathbf{G}_i = \left(\frac{T_0^2}{L_0} - \frac{\pi L_0^2 T_0^2}{6 M_0} \frac{d_i^3}{m_i} \rho \right) \mathbf{g}, \quad R_i = 3\pi\mu \frac{L_0 T_0}{M_0} \frac{d_i}{m_i}, \quad (21)$$

the final form of the equation of motion of a particle in a liquid is obtained as:

$$\frac{d\mathbf{w}_i}{d\tau} = G_i - R_i \mathbf{w}_i, \quad (22)$$

5. Initial conditions, finite difference scheme and calculation algorithm

5.1. Initial conditions

Let us consider two types of particles in a liquid, namely filler and polymer macromolecules. Each type of particles has own normal distribution of masses, diameters and densities. All particles are distributed in the liquid at the initial time uniformly and with zero velocities. Let us denote the number of particles of the first and second types as N_1 and N_2 . The total number of particles is $N = N_1 + N_2$.

Let us consider the distribution function:

$$f_{\text{Gauss}}(f_{\text{avg}}, f_{\text{disp}}) = f_{\text{avg}} + f_{\text{disp}} \cdot \sqrt{-2 \cdot \ln(\text{rnd}(1))} \cdot \cos(2\pi \cdot \text{rnd}(1)), \quad (23)$$

where f_{avg} is a mean, f_{disp} is a dispersion, and $\text{rnd}(1)$ is random value generator in the range $[0, 1]$.

Let us enumerate all particles so that the first N_1 particles are particles of the filler – the first type particles, and the next N_2 particles are particles of the polymer macromolecules – the second type particles. The particle size and density distribution are described as:

$$d_i = \begin{cases} f_{\text{Gauss}}(d_{T1}, \sigma_{dT1}), & 1 \leq i \leq N_1 \\ f_{\text{Gauss}}(d_{T2}, \sigma_{dT2}), & N_1 < i \leq N_1 + N_2 \end{cases}, \quad \rho_i = \begin{cases} f_{\text{Gauss}}(\rho_{T1}, \sigma_{\rho T1}), & 1 \leq i \leq N_1 \\ f_{\text{Gauss}}(\rho_{T2}, \sigma_{\rho T2}), & N_1 < i \leq N_1 + N_2 \end{cases}, \quad (24)$$

where d_{T1} and d_{T2} are average diameters of particles, σ_{dT1} and σ_{dT2} are dispersions of diameters, ρ_{dT1} and ρ_{dT2} are average densities of particles, $\sigma_{\rho T1}$ and $\sigma_{\rho T2}$ are dispersions of densities. Knowing the diameters of the particles, we can determine their masses. It allows

calculating the dimensionless equation coefficients for each particle from (21).

5.2. Finite-difference scheme

The equation (22) in finite-difference form is:

$$\frac{w_i^{n+1} - w_i^n}{\Delta\tau} = (1 - \theta)(G_i + R_i w_i^n) + \theta(G_i + R_i w_i^{n+1}), \quad (25)$$

where $\theta \in [0, 1]$ is a finite-difference scheme parameter [25].

The finite-difference relation allows calculating the velocity of a particle in the next moment of time:

$$w_i^{n+1} = \frac{(1 + (1 - \theta)\Delta\tau R_i)w_i^n + \Delta\tau G_i}{(1 - \theta\Delta\tau R_i)}, \quad (26)$$

Equation (26) also allows determining the coordinate of the particle using similar finite-difference relations.

5.3. Calculation algorithm

The computational algorithm was implemented based on the well-known finite element method [28]. The use of this method for calculating the sedimentation rate is discussed in detail in the works [29,30].

On the basis of a mathematical model, a computer program was written. The program works according to the following algorithm. In the beginning, all the parameters of the task are set at the initial conditions. After that, the computational cycle of time integration is started. At the first step, the velocities and coordinates of all particles are calculated according to the individual of motion, which describes the motion of a particle without interactions and influence of thermal motion of a liquid (26). At the second step, taking into consideration the influence of the Brownian (thermal) motion of a liquid, the recalculation of the particle

velocities is fulfilled. At the third step, the collisions of the particles are calculated taking into consideration that one particle can have only one collision with the other one on each integration step. At the final step, the concentration of particles in the laser beam area is calculated.

6. Calculation results and verification

The numerical calculation is carried out for the sedimentation of two types of particles – aluminum oxide and polymer macromolecules in ethyl acetate. The density of ethyl acetate is $\rho_{T1} = 902 \text{ kg/m}^3$, its viscosity is $\mu = 0.40016 \times 10^{-3} \text{ Pa}\cdot\text{s}$. The density of the first type particles (heavy, aluminum oxide Al_2O_3) is $\rho_{T1} = 7987 \text{ kg/m}^3$. The density of the second type particles (light, polymer macromolecules) is $\rho_{T1} = 3000 \text{ kg/m}^3$. The basic size of the first type particles is $d_{T1} = 0.25 \times 10^{-6} \text{ m}$, and of the second type particles is $d_{T1} = 0.125 \times 10^{-6} \text{ m}$. The number of the first type particles is taken equal to 1000, and of the second type particles is 10,000.

The estimation results of maximum velocities of the particles are presented in Fig. 2. The dependence of the maximum sedimentation velocity of particles with a diameter of 250 nm is shown by the red line, and for the particles with a diameter of 125 nm is shown by the blue line.

Obviously, if the density of a particle coincides with the density of the liquid, the velocity of sedimentation is equal to zero. With an increase of the density of particles, their mass increases also, it leads to an increasing sedimentation velocity. The limitation of the maximum sedimentation velocity is caused by the liquid resistance forces, which depend on the square of the particle diameter, but the mass of the particle depends on the cube of the diameter, which means that larger particles settle faster than smaller ones.

The normal (Gaussian) distribution of particle sizes and densities is taken into account. For particles of the

filler (Al_2O_3), the dispersion of the diameters distribution is chosen equal to 1.5×10^{-2} , the dispersion of the density is chosen equal to 4.0×10^{-2} . For the polymer macromolecules, the dispersion of the diameter distribution is chosen equal to 3.0×10^{-2} , and the dispersion of the density distribution is chosen equal to 2.0×10^{-2} . The temperature of the cuvette boundaries is considered constant and equal to 300 K. The diameter of the particle concentration control window is 0.01 m; the control window is located in the middle of the cuvette horizontally and at a height of 0.035 m from the lower boundary. The effect of Brownian motion of liquid molecules on the velocity and movement of the deposited particles is taken into account on the basis of the elastic collision model. The speed of Brownian motion of liquid molecules is calculated, while the molar mass of ethyl acetate is taken to be $18.0 \times 10^{-3} \text{ kg/mol}$. Only the model of inelastic collisions of particles with each other is taken into account, in which the particles stick together completely, forming a new particle with a new mass and velocity.

The results of the calculation of total light obscured by particles via Rayleigh scattering in the area of the laser beam are shown in Fig. 3 by red, blue and violet lines. The derivative of light intensity changing is shown by pink line in Fig. 3. As can be seen from the concentration dependences in Fig. 3, with the start of the process, the sedimentation of heavy particles occurs initially and very quickly, after which the sedimentation of light particles of the second type occurs. We carried out the series of experiments on the sedimentation of polymer-coated particles of aluminum oxide in ethyl acetate.

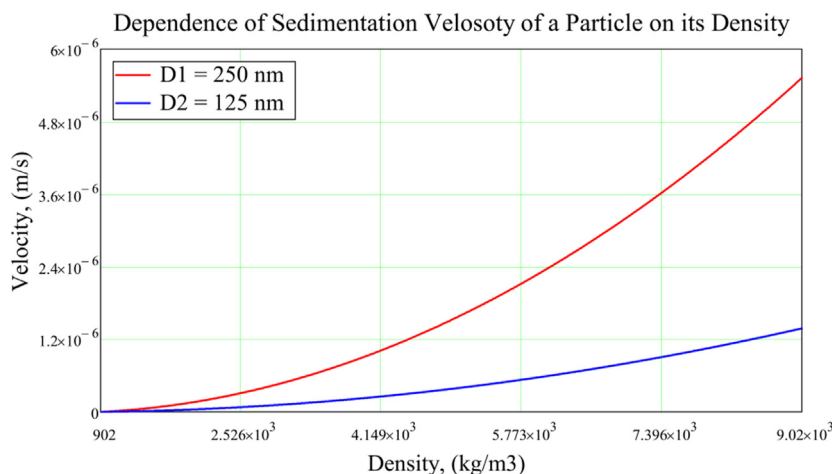


Fig. 2. The dependence of the sedimentation velocity of particles on their density and diameter: (red line is used for the particles with a diameter of 250 nm, and blue line is used for the particles with a diameter of 125 nm).

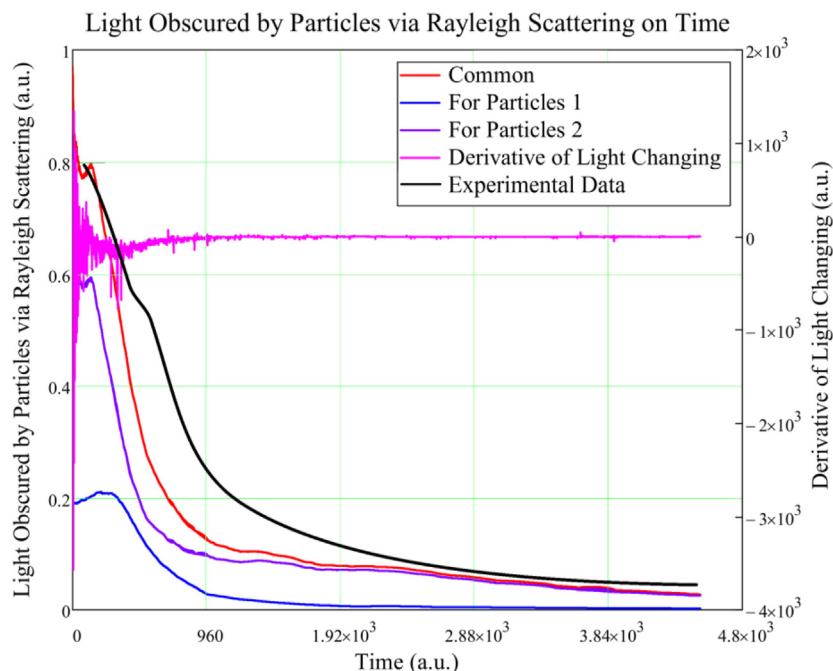


Fig. 3. Changing total light obscured by particles via Rayleigh scattering in the area of the laser beam versus time.



Fig. 4. The experimental setup.

The Fig. 4 shows the experimental setup photo. The experimental data results in the above described conditions are shown in Fig. 3 by black line.

The good correlations between experimental and modeling data can be observed by comparing data in Fig. 3. The differences between experimental and computing results explained by the limitations of the mathematical model formalization, the possible particle agglomeration, and the experimental conditions. However, we did not set the task of determining the molecular weight of the polymer shell with high

accuracy in this work. The obtained calculation results provide an approximate range of mechanical properties of the polymer shell of the encapsulated particles. This is sufficient to reduce the number of solutions of the polymer mechanics inverse task, and, thereby, to solve the problem of uniqueness of its solution.

7. Conclusions

The method for estimating the molecular weight of the polymer macromolecules in shells on the surfaces of nanoparticles is proposed. Unlike the traditional methods for the measuring of polymer molecular weight [31,16,32], the proposed method does not require a separation of a solution into fractions containing separate nanoparticles and polymer macromolecules. It should be noted that the physical feasibility of photo sedimentation for measuring the molecular weight of polymers was substantiated in the work of Debye in 1947 [16]. However, during measurements, it is required to ensure the constant temperature and the volume of solution. The investigation of the mathematical model of the sedimentation of nanoparticles of two types and the experimental results confirm the feasibility of the proposed method. The results and estimations allow us both to determine the sedimentation time and to formulate the method requirements for measuring particles of various sizes and

densities. The calculation results are in good correlation with the experimental data. It confirms the correctness of the choice of the mathematical model and its numerical implementation. The proposed approach can be used to create equipment for nanoparticle parameters (mass, density) measuring.

Conflict of interest

No conflict of interest among authors.

Acknowledgements

A.Zh. Sakhabutdinov and O.G. Morozov was funded by Ministry of Science and Higher Education of the Russian Federation (Agreement No. 075-03-2020-051/3, topic No. fzs-2020-0021) in part of physical task formulation, data and results verification. M.P. Danilaev was funded by Ministry of Science and Higher Education of the Russian Federation (Agreement No. 075-03-2020-051, topic No. fzs-2020-0020) in part of mathematical model construction, training and tuning, and realization.

References

- [1] S.Z. Al Sheheri, Z.M. Al-Amshany, Q.A. Al Sulami, N.Y. Tashkandi, M.A. Hussein, R.M. El-Shishtawy, The preparation of carbon nanofillers and their role on the performance of variable polymer nanocomposites, *Des Monomers Polym* 22 (2019) 8–53, <https://doi.org/10.1080/15685551.2019.1565664>.
- [2] S.M. Rahimian-Kolour, H. Moshrefzadeh-Sani, M.M. Shokrieh, S.M. Hashemianzadeh, On the behavior of isolated and embedded carbon nano-tubes in a polymeric matrix, *Mater Res Express* 5 (2018) 25019, <https://doi.org/10.1088/2053-1591/aaac4e>.
- [3] H.K. Kim, I.W. Nam, H.K. Lee, Enhanced effect of carbon nanotube on mechanical and electrical properties of cement composites by incorporation of silica fume, *Compos Struct* 107 (2014) 60–69, <https://doi.org/10.1016/j.compstruct.2013.07.042>.
- [4] L. Shi, Y. Lu, Y. Bai, Mechanical and electrical characterisation of steel fibre and carbon black engineered cementitious composites, *Proc Eng* 188 (2017) 325–332, <https://doi.org/10.1016/j.proeng.2017.04.491>.
- [5] M. Sánchez, M. Campo, A. Jiménez-Suárez, Ureña, Effect of the carbon nanotube functionalization on flexural properties of multiscale carbon fiber/epoxy composites manufactured by VARIM, *Compos B Eng* 45 (2013) 1613–1619, <https://doi.org/10.1016/j.compositesb.2012.09.063>.
- [6] A.K. Cholker, M.A. Tantray, Influence of carbon fibres on strain sensing and structural properties of RC beams without stirrups, *Karbala Int J Modern Sci* 6 (2020) 129–140, <https://doi.org/10.33640/2405-609X.1389>.
- [7] S. Lurie, P. Belov, D. Volkov-Bogorodsky, N. Tuchkova, Interphase layer theory and application in the mechanics of composite materials, *J Mater Sci* 41 (2006) 6693–6707, <https://doi.org/10.1007/s10853-006-0183-8>.
- [8] S. Tabasum, M. Younas, M. Zaeem, I. Majeed, M. Majeed, A. Noreen, M. Iqbal, K. Zia, A review on blending of corn starch with natural and synthetic polymers, and inorganic nanoparticles with mathematical modeling, *Int J Biol Macromol* 122 (2019) 969–996, <https://doi.org/10.1016/j.ijbiomac.2018.10.092>.
- [9] I.A. Budkute, B.E. Geller, L.A. Shcherbina, Experimental study of the structure of polyacrylonitrile gel fibres, *Fibre Chem* 36 (2004) 358–364, <https://doi.org/10.1007/s10692-005-0009-5>.
- [10] S.V. Panin, Y.P. Stefanov, P.S. Lyubutin, Estimation of meso-scale strain with fatigue crack propagation through quantitative analysis of displacement vector fields by a television-optical measuring complex, *Phys Mesomech* 13 (2010) 88–95, <https://doi.org/10.1016/j.physme.2010.03.011>.
- [11] K. Shimizu, T. Miyata, T. Nagao, A. Kumagai, H. Jinnai, Visualization of the tensile fracture behaviors at adhesive interfaces between brass and sulfur-containing rubber studied by transmission electron microscopy, *Polymer* 181 (2019) 1–6, <https://doi.org/10.1016/j.polymer.2019.121789>.
- [12] A.A. Akhmadeev, E.A. Bogoslov, M.P. Danilaev, M.A. Klabukov, V.A. Kuklin, Influence of the thickness of a polymer shell applied to surfaces of submicron filler particles on the properties of polymer compositions, *Mech Compos Mater* 56 (2020) 241–248, <https://doi.org/10.1007/s11029-020-09876-4>.
- [13] D. Balköse, Influence of filler surface modification on the properties of PP composites, in: *Surface Modification of Nanoparticle and Natural Fiber Fillers*, John Wiley & Sons, Ltd., 2015, pp. 83–108, <https://doi.org/10.1002/9783527670260.ch4>.
- [14] M. Gazzola, L.H. Dudte, A.G. McCormick, L. Mahadevan, Forward and Inverse Problems in the Mechanics of Soft Filaments, vol. 5, *Royal Society open science*, 2018, pp. 1–35, <https://doi.org/10.1098/rsos.171628>.
- [15] A.M. Elert, R. Becker, E. Duemichen, P. Eisentraut, J. Falkenhagen, H. Sturm, U. Braun, Comparison of different methods for MP detection: what can we learn from them, and why asking the right question before measurements matters? *Environ Pollut* 231 (2017) 1256–1264, <https://doi.org/10.1016/j.envpol.2017.08.074>.
- [16] P. Debye, Molecular-weight determination by light scattering, *J Phys Chem* 51 (1947) 18–32.
- [17] D. Campbell, R.A. Pethrick, J. White, *Polymer Characterization: Physical Techniques*, CRC press, 2017.
- [18] O. Akbulut, C.R. Mace, R.V. Martinez, A.A. Kumar, Z. Nie, M.R. Patton, G.M. Whitesides, Separation of nanoparticles in aqueous multiphase systems through centrifugation, *Nano Lett* 12 (2012) 4060–4064, <https://doi.org/10.1021/nl301452x>.
- [19] J.D. Robertson, L. Rizzello, M. Avila-Olias, J. Gaitzsch, C. Contini, M.S. Magoñ, S.A. Renshaw, G. Battaglia, Purification of nanoparticles by size and shape, *Sci Rep* 6 (2016) 1–9, <https://doi.org/10.1038/srep27494>.
- [20] J. Midelet, A.H. El Sagheer, T. Brown, A.G. Kanaras, M.H. Werts, The sedimentation of colloidal nanoparticles in solution and its study using quantitative digital photography, *Part Syst Char* 34 (2017), <https://doi.org/10.1002/ppsc.201700095>.
- [21] C. Minelli, A. Sikora, R. Garcia-Diez, K. Sparnacci, C. Gollwitzer, M. Krumrey, A.G. Shard, Measuring the size and density of nanoparticles by centrifugal sedimentation and flotation, *Analytical Methods* 10 (2018) 1725–1732, <https://doi.org/10.1039/c8ay00237a>.
- [22] J.R. Martin, J.F. Johnson, A.R. Cooper, Mechanical properties of polymers: the influence of molecular weight and molecular

- weight distribution, *J Macromol Sci Rev Macromol Chem* 8 (1972) 57–199, <https://doi.org/10.1080/15321797208068169>.
- [23] P. Bracco, A. Bellare, A. Bistolfi, S. Affatato, Ultra-high molecular weight polyethylene: influence of the chemical, physical and mechanical properties on the wear behavior, A review, *Materials* 10 (2017) 791–802.
- [24] S. Hussein, O. Morozov, M. Danilaev, V. Kuklin, A.V. Anfinogentov, S.A. Zh, G.I. Sakhabutdinova, A mathematical model for measuring the concentration of nanoparticles in liquid during their deposition, *Meždunarodnyj naučno-issledovatel'skij žurnal (International Research Journal)* 12 (2020) 94–107.
- [25] Z. Sahabutdinov, *The Analysis of Discrete Models of a Particle Movement*, IMM RAN, Kazan, 1995.
- [26] P. Kondratenko, *Theoretical Fundamentals of Hydrodynamics and Heat Transfer*, Nuclear Safety Institute, RAS, Moscow, 2003.
- [27] A. Mazo, K. Potashev, *Hydrodynamics: Textbook. A Guide for Non-mathematical Students Faculties*, Kazan. un-t, Kazan, 2013.
- [28] O.C. Zienkiewicz, R.L. Taylor, J.Z. Zhu, *The Finite Element Method: its Basis and Fundamentals*, Elsevier, 2005.
- [29] J.M. Hervouet, *Hydrodynamics of Free Surface Flows: Modelling with the Finite Element Method*, Wiley, New York, 2007.
- [30] R.M. MacMeccan, J.R. Clausen, G.P. Neitzel, C.K. Aidun, Simulating deformable particle suspensions using a coupled lattice-Boltzmann and finite-element method, *J Fluid Mech* 618 (2009) 13–39, <https://doi.org/10.1017/S0022112008004011>.
- [31] W. Li, H. Chung, C. Daeffler, J.A. Johnson, R.H. Grubbs, Application of 1H DOSY for facile measurement of polymer molecular weights, *Macromolecules* 45 (2012) 9595–9603, <https://doi.org/10.1021/ma301666x>.
- [32] N.S. Othman, G. Févotte, D. Peycelon, J.B. Egraz, J.M. Suau, Control of polymer molecular weight using near infrared spectroscopy, *AIChE J* 50 (2004) 654–664, <https://doi.org/10.1002/aic.10059>.